Steels Specimens' Inspection with Structured Light Scanner

Árpád József Somogyi[1*], Tamás Lovas[1], Ákos Szabó-Leone[2], András Fehér[2]

[1] Department of Photogrammetry and Geoinformatics, Faculty of Civil Engineering, Budapest University of Technology and Economics, Műegyetem rkp. 3., H-1111 Budapest, Hungary
[2] 4iG Plc, Montevideo u. 8., H-1037 Budapest, Hungary
[*] Corresponding author, e-mail: somogyi.arpad@emk.bme.hu

Abstract
With the recent rapid advances in technology, the use of 3D scanning systems in the engineering world has become more and more prevalent thanks to the ease of use, the improved data collection process, and the increase in the accuracy of the acquired data. During the rebuilding of the Tisza bridge on the M4 motorway, the contractor discovered that the plates used to build the steel superstructure had developed corrosion damage during several years of storage. Plates with a tolerable level of corrosion were intended to be used, but the question was how the increased surface roughness will affect the fatigue life of the plates and the welded steel fabrications made from the plates. As part of this test, fatigue specimens were measured from the material to be used for the bridge and welded with two different geometries with the help of a structured light 3D scanner (SLS scanner). This paper discusses the measurement and inspection of these steel specimens of a highway bridge, before and after the fatigue test of the parts. From the acquired data we examined defects on the surface of the parts, physical deformations by comparing measured data to a CAD model and calculated the amount of material which was lost during stress testing.

Keywords
structured light scanner, 3D model, geometry inspection, steels specimens

1 Introduction

3D scanners have been around since the 60s, but for a long period the results that it could deliver was not up to par with what Coordinate Measuring Machines (CMM) would offer. Today's structured light 3D scanning technologies are among the most reliable, non-invasive and cost-effective object acquisition techniques [1–8].

One example to illustrate the cost and time effectiveness of this technology are the general constructors in the USA who are increasingly using 3D scanning to detect deviations from the building information modelling (BIM) during the construction process. The McCarthy Building Company in the New Stanford Hospital in Palo Alto (CA) used Faro scans to control 1331 meter of overhead steel structure in 13 man-hours, providing data of the 100% of the structure's surface, while with traditional technology the estimated time would have been 64 man-hours to capture 3 points on each main beam [9].

3D scanners, which use near visible light, are optimized to work with opaque objects, which reflect the light in an unorganized manner in all directions, called also diffuse reflection, so; despite the continuous technology development there are still substantial limitations in digitalizing certain surfaces. The most problematic non-cooperative surfaces are the transparent, translucent, shiny, reflecting, specular and black surfaces. Apart from these, edges, grooves, bores, and milled surface also present complications for the scanner to capture.

The manufacturing industry needs rapid and high-fidelity methods to scan difficult surfaces, which can be integrated in production lines. In 2010 Ihrke did an overview of acquisition approaches for such surfaces. The conclusion was that although there are technologies, which can handle rather well certain challenging surfaces, the algorithms that enable producing the surface models are still not generally applicable. Until 2014 none of these technologies were applied in commercial systems [10].

In the case of non-cooperative surfaces, the simplest solution, although not applicable in every situation, is still the use of antireflective coating. The majority needs to be wiped off but there are volatile ones too. Here are some of the commonly used ones:

Helling GMBH produces 3D Laserscanning Anti-Glare Spray, the most used one in Europe, free of acetone, talc and dangerous chemicals and wipes off easily. Magnaflux produces Spotcheck® SKD-S2, a fast-drying non-volatile aerosol that provides a uniform, matt, anti-glare finish. Multiple layers can be built with minimal thickness, but it is not suitable for porous surfaces. Kremer Pigmente produces the Cyclododecane Spray, a very volatile substance that sublimes, eliminating additional steps for removal. The only limitation is due to its solvent-based nature, thus can't be used to scan plastic objects. Finally, a new product from 2019 the volatile Blue spray from AESUB, which evaporates faster than cyclododecane sprays and has less odor. Although white light was the go-to technology for years, now the blue light is the most indicated for some kind of challenging surfaces. Compared to white light scanners, LEDs used by blue light scans are more consistent, assure longer working hours and are less sensitive to heat. Producers claim that thanks to the short wavelengths of the color blue, they can successfully scan shiny and slightly transparent surfaces [11]. However, these kinds of problems are not unique to SLS measurements; Lovas et al. [12] report on dealing with difficult-to-measure dark surfaces during terrestrial laser scanner measurements of a race boat.

Some software with advanced algorithms, like Artec Studio or OptoCat, claim to be able to scan shiny and black surfaces, by adjusting the sensitivity of the scanner, and eventually the scanning angle and distance

Structural light scanners are used in areas requiring high accuracy measurements. The Aviation Missile Research Development & Engineering Centre (AMRDEC) has been using extensively ATOS blue light scanners for high detail scanning since 2017. The fields of application range from reverse engineering to detection of deviations respect to the original design.

In the process to determine the cause of failure, NASA used ATOS white light scanners to scan complex shape debris of the left wing of the Colombia Space Shuttle [13, 14].

Somogyi et al. [15] used an SLS-scanned model as a reference surface to investigate the measurement results from different 3D measurement techniques. Sengoz et al. [16] investigated the applicability of 3D scanning to the texture of asphalt concrete pavements, which have been validated using mature measurement techniques.

2 Equipment and specimens

As we have seen, there are many surfaces that pose difficulties while being scanned using visible light. In this research we were presented with two types of shiny surfaces, the fatigue test subjects had shiny welded surfaces while the tension test subjects had their edges as shiny surfaces as an effect of the cutting of the original steel sheets.

When the scanning target has homogeneous surfaces, it will present a problem for the software when it is trying to align the different scans. This is due to the fact that the software isn't able to distinguish the difference between similar surfaces and will decide that they are in fact the same.

We used AICON SmartSCAN 3D, which is a high-end compact industrial scanner [17]. It is composed by two digital cameras and a pattern projector arranged in an arm. The light source is a white or blue LED. The digital cameras of this scanner have a resolution of 5 or 8 megapixel. Measurement fields range from 60 mm to 1550 mm. The projector casts a black-and-white pattern onto the object being scanned, which supports obtaining an accurate result. While this pattern is being projected, both cameras at each end of the scanner capture images which the computer will then use to calculate the point coordinates, resulting in a 3D model of the object. For this task we decided to use M450 FOV optics on the cameras as these allows us to scan surfaces big enough (335 × 280 mm) with each scan which facilitates the final alignment process while not losing on precision.

A total of 17 steel specimens were scanned, from which 8 were going to be subjected to a fatigue test and 9 to a tensile stress test. The first group of 8 test subjects had strengthening joints welded on them, 4 vertical joints and 4 horizontal joints. The parts' dimensions were approximately 500 mm × 60 mm × 14 mm. The second group were cut from a 440 mm high, 14 mm thick sheet, with a final approximate dimension of 400 mm × 60 mm × 14 mm.

It was important to execute an accurate scan of each part, which means that every portion that is relevant to create a complete mesh, should be visible and in the correct position. To achieve this goal, the parts should be positioned in a holder so that both sides of it can be scanned in one cycle.

On some occasion we were presented with a big homogeneous surface, a table for example, with lots of portions that are rather similar to each other, disabling the alignment with no markers. In our case the surface and edges of the parts were akin to each other, in consequence we used markers to facilitate the process of alignment of each scan. Apart from the markers, because of the parts surface properties, we also had to apply a couple of layers of antireflective coating onto them in aerosol form; these coatings build minimal thickness and are easily washed off with water and detergent [18].

2.1 Scanning environment

There are a few aspects that can hinder the scanning process, namely:

- The environment where we are scanning.
- The surface quality of the object. Is it black, maybe shiny, reflective, or transparent? If so, there is a need to choose a method to bypass the difficulties i.e., anti-reflection aerosols, from which there are two kinds, sublimating and non-sublimating.
- Because of homogeneous surfaces on the specimens, we need to help the software to orientate itself when it is aligning the scans.
- The deciding factors for choosing the optics on the cameras are: the size of the object, the aimed accuracy and the measurement time.

In our case a room with concrete floor was chosen for the scanning; the scanner is mounted on top of a stand which makes it more sensitive to the floor vibration, so top floors that have bases that are able to transmit the vibration generated by people walking, can't be worked with. The other important factor when choosing the scanning environment is to pick a location where you are able to provide the ambient darkness; this is done so that only the projectors light hit the inspected specimen and the patterns projected onto it are clearly visible for both cameras.

2.2 Setup and calibration

The scanning process starts out by setting up the scanner on its stand; connecting it to its control unit and adapter, and these to the laptop from which we control the process. The equipment is switched on in a specific sequence, otherwise it could damage the scanner. The sequence is as follows, first the scanner is turned on, then the control unit, the adapter and finally the laptop.

The SmartSCAN 3D comes with its own software called OptoCat. As mentioned before, the optics that were chosen for the measurement of the subjects were the M450. Setting these up meant that the scanner had to be recalibrated, this was done by using the calibration panel that was provided with the scanner. The instrument captured said board in different positions, specified by OptoCat, to recalibrate itself.

2.3 Measurement process

After the calibration, a holder was fixed onto the turn table to keep the specimens vertical and stable during the scanning process. The software offers a variety of scanning options from using a robot, to manually doing each scan. For our task, the Automatic Measurement option was chosen which allows us to fully automatize a scanning cycle with the help of the turntable.

Inside the project parameters we made sure to specify the filtering out of overexposed pixels which created noise on the surface of the objects after the scanned data went through the meshing process. The data quality was also ensured by prioritizing the mesh boundary line.

A high number of captures per cycle ensures more data which result in more precise outcome while sacrificing time. For physically complex object having edges, milled surfaces, grooves, shiny surfaces, etc. a large quantity of scans is required to obtain the best quality possible. The optimal number of scans was concluded to be 8, as it captured the complete physical form of the objects without sacrificing too much time.

The OptoCat software comes with a function that allows us to teach the program the position and rotation axis of the surveyed object. This enables the program to automatically align the later captured scan automizing a process which in other cases would have to be done manually (such as during the scanning of large objects where a turntable is not an option). The scanner head was set to a vertical position so that the right camera was on top of the left one. The reason for this is that both cameras are positioned in a 27° angle from each other and OptoCat will only represent data that both cameras are able to see. If there is a surface one of the cameras doesn't see, data won't be captured from it.

The starting position of the cameras' focus was on the top edge of the vertically positioned subject, with the cameras looking down to it. This is done so that both cameras could see the top face of the object. With the first 8 scans ready we ran them through an aligning process inside the software that would go over each capture and search for similarities. These similarities are then used to align the point cloud, our aim with this procedure is to eliminate convergence between the scans and reduce the RMS to as low as possible. After the first alignment process, the scans were used as a reference for the further measurements. For the next rotation, the scanner head was moved down so the focus of the cameras fell on the middle of the object. Another set of 8 scans was finished and aligned to the first batch. From here the parts were taken out of the holder and rotated so the previously bottom face was on top, meanwhile the scanner stayed in its current position. Since the position of the object changed, relative to the

table, it had to be considered in the measurement. From this point the same process as described before has been redone but this time from middle to the top of the specimen. In the case of the very first scan that was done after changing the position of the sample, a manual alignment was necessary to indicate the new orientation for the automatic alignment. For each sample a total of 32 scans were done, and at the end all of them were subjected to an alignment with the very first scan being the only one to remain locked as a reference to the others to align onto. The last steps were to load in the scans in their Full resolution and then we deleted the holder that was captured during the scanning process. The next step after the clean-up was to merge all the scans and create a mesh from them by triangulating the point cloud.

2.4 Results

The results were a total of 17 meshes which were loaded one by one into Geomagic Wrap [19]. This software transformed our data and rendered it usable for the inspection. The following steps were executed:

- The markers were selected and cut out from the mesh. The leftover holes were filled in with fill hole tangentially function, which matches the surrounding mesh curvature.
- The samples were then aligned onto a predefined coordinate, this was done by selecting one of the extreme edge points of the object to then create 3 planes on the neighboring faces. Using these planes, we defined the XY, XZ and YZ plane.

After the fatigue test, 4 of the original 8 specimens came back broken into two parts. For the transversely welded samples, they broke on one of the welded sides resulting in 55/45 parts of the original object. As for the longitudinally welded pieces, they broke on one of the ends of the welding resulting in 70/30 pieces. Since the broken surfaces were too shiny, we had to apply antireflection coating on them to avoid noise in the scans. From here the scanning process and the data processing was the same as that of before the stress test

In the case of the 9 samples subjected to a tension test, 4 broke into two and 5 remained intact but suffered physical deformation, but we also got 3 new samples from which one broke into two pieces and 2 deformed. Just like for the fatigue tested specimens, we applied antireflective coating on the broken surfaces and the elongated surfaces and scanned the parts once more (Fig. 1).

The result was a total of 8 new fatigue tested mesh and 17 tension tested mesh. The next step is the inspection process, where we compared the original state of the samples to their after-test state as shown in Fig. 2, and in the case of the tension tested samples, we also compared both the original and the deformed states to an ideal CAD model. This model was created inside Geomagic DesignX, which is a reverse engineering software using the scanned mesh as data to reconstruct our sample [20]. The inspection was done using Geomagic ControlX which is specifically used to do inspection processes between reference data and measured data [21].

In the case of the fatigue tested samples we used their original state as reference, as for the measured data, both sides of the broken object were imported and aligned together using the reference data (Fig. 3). By using the Transformation Alignment, we manually aligned the measured data on top of our reference and with the Best Fit Alignment a fine alignment was executed additionally to minimize the overall deviation, resulting in what is shown in Fig. 4. We deemed these two functions to be the best for the inspection based on aligning accuracy, nevertheless the software also offers other solutions that could have been used.
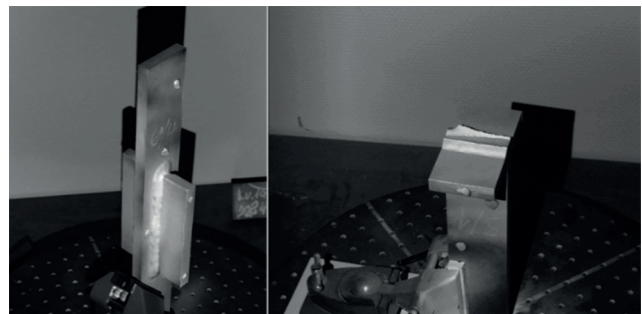
Fig. 1 Subjects before and after the fatigue test
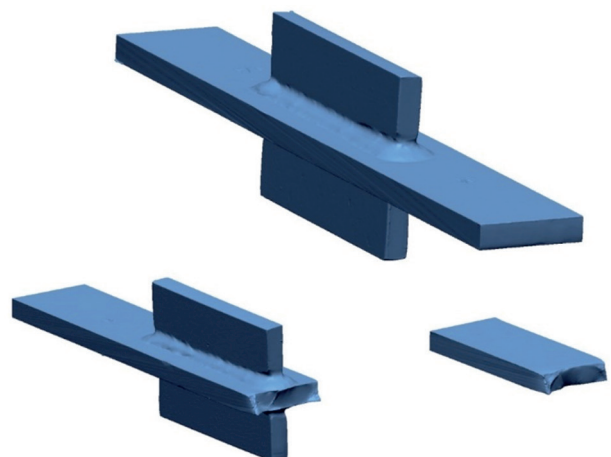
Fig. 2 Fatigue tested sample mesh before and after test
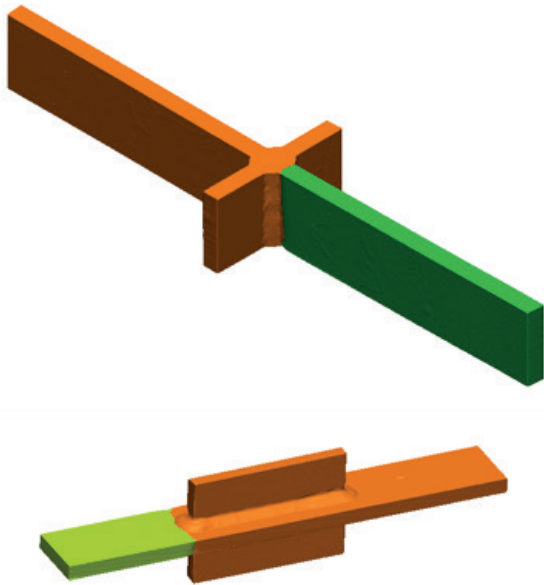
Fig. 3 The aligned broken parts of the welded specimens
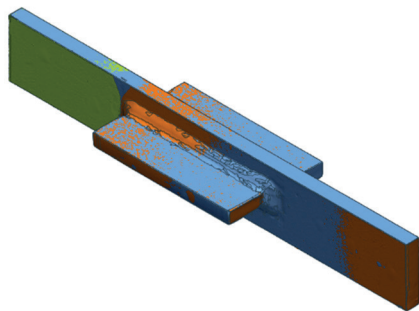
Fig. 4 The original mesh (blue) was used as the reference to align both meshes after the fatigue test

Fig. 5 3D color map created from the 3 meshes (2 broken parts of the specimen compared to its original state) showing the deviations between reference and measured data

A 3D color map was created as shown in Fig. 5, to represent the deviations on the specimens. The Min and Max ranges, which limit the range of the deviation analysis, were set to –1 and +1 mm. The tolerance used was set to a specific value of ±0.05 mm because there wasn't notable deviation going over those bounds.

After creating the deviation map on top of the reference, by using the 2D Compare function a set of deviation analyzing section profiles were created on the scanned object. For this group of samples, they were only sectioned on the Y-axis and the Z-axis as the X-axis didn't provide any further information. A total of 6 cross-sections were created along the Y-axis and 5 along the Z-axis. Inside each cross-section we selected points along the profile which provides two important pieces of information: the gap distance between the reference and measured data, and a color representation of approval based on if the gap exceeds the given tolerance. The number of points picked depends on the average range of deviation on all the cross-sections of a given axis. In the case of the Y-axis, because the profile covered a larger area on the sample, there was a need for more points as there were going to be more changes in the deviation. The positions of the inspection points were:

- The places where the part broke off. A larger concentration of points is present where the part broke as larger gaps can be seen there.
- Areas showing large deviations.
- Areas at the extremes of the test samples.

The results of the 2D Compare were graphs of the cross-sections (Fig. 6) with their respective inspection points and a table where the information was organized to make it easier to go through.

In case of our tension tested specimens, we used a total of 15 cross-section cutting planes for every inspection, 3 along the Z-axis, 5 along the X-axis and 7 along the Y-axis. This was done so that we could:

- Inspect the extreme ends on the part
- Inspect the narrow neck section of the part

In Fig. 6 we can see the result of comparing the two pieces of a broken specimen to its original state. At the labelled point "6/4_YY_4:1" a big jump in the gap distance between reference and measured data can be observed, this is due to the part losing some of its material during the fatigue test.

The first comparison was between the CAD model and the original state of the parts in order to find out if there were deformations already present on the test subjects. Next, every broken off piece and deformed part that was still intact was compared to the CAD model to see what changes could be seen after the test.
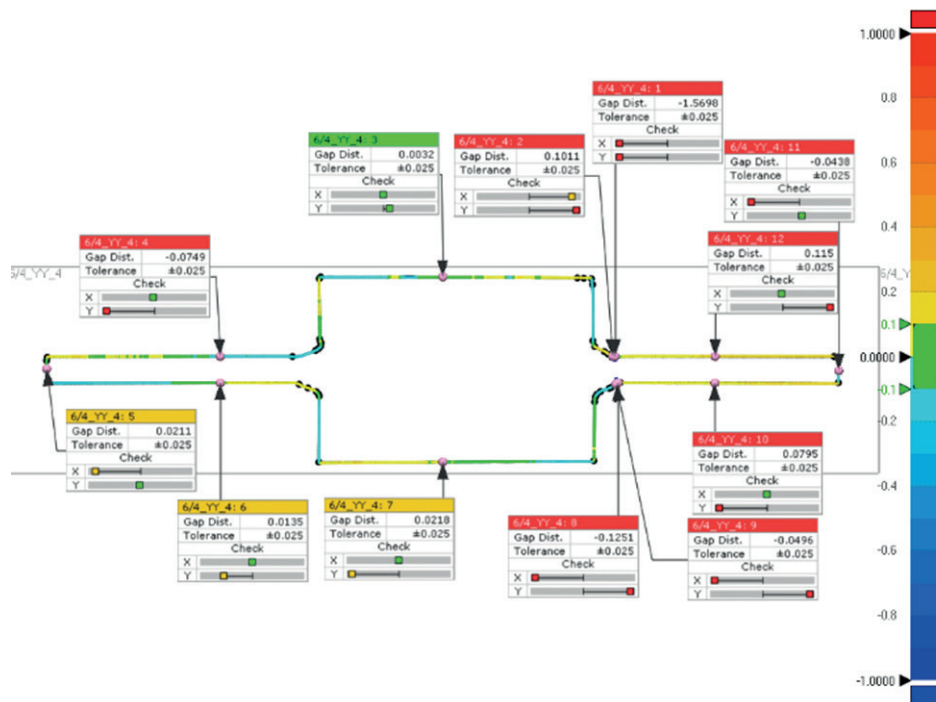
Fig. 6 Cross-section of a fatigue tested steel part

3 Conclusions

The presented results show how advanced are the solutions that high accuracy 3D surveys provide for engineering thanks to the rapid advancements in the structured light scanner technologies. With the combination of white-light based scanning and quality–control tools we are able to provide highly accurate geometric data (the digital twin of the specimen), for which the human error can be minimalized. The entire surface of the object can be digitalized regardless of the complexity of its geometry, even parts that pose complications to scan are measurable (holes, tunnels, grooves, cracks) from additional scan positions. In case of regular and simple object like the scanned steel specimens, the measurement can be automatized. The outcome of the measurement process is a complete surface model (the objects digitalized copy), which enables to take as many cross-sections and inspection points as needed without additional physical measurements. On these bases, a semi-automatic report can be generated from the data where user defined inspection points are plotted from which the deviation values are presented in a structured table. The produced 3D deviation maps and the 2D sections provide easily understandable information for disciplines such as welders and steel construction engineers. The measurement and inspection methods presented in this article demonstrates that they are easily standardizable and the produced results are objective. In compliance with the scanning environment requirements, even in the case of difficultly measured surfaces we are able to reach high geometric accuracy.

Acknowledgement

References

[1] Valkenburg, R. J., McIvor, A. M. "Accurate 3D measurement using a structured light system", Image and Vision Computing, 16(2), pp. 99–110, 1998.
https://doi.org/10.1016/S0262-8856(97)00053-X

[2] Legarda-Sáenz, R., Bothe, T., Jüptner, W. P. O. "Accurate procedure for the calibration of a structured light system", Optical Engineering, 43(2), 464, 2004,
https://doi.org/doi: 10.1117/1.1635373

[3] Begley, C. "Structured Light Scanning", In: The Encyclopedia of Archaeological Sciences, Wiley, 2018. ISBN: 9780470674611
https://doi.org/10.1002/9781119188230.saseas0560

[4] Eiríksson, E. R., Wilm, J., Pedersen, D. B., Aanæs, H. "Precision and Accuracy Parameters in Structured Light 3-D Scanning", The International Archives of the Photogrammetry, Remote Sensing and Spatial Information Sciences, XL-5/W8, pp. 7–15, 2016.
https://doi.org/10.5194/isprs-archives-XL-5-W8-7-2016

[5] Freeman Gebler, O., Goudswaard, M., Hicks, B., Jones, D., Nassehi, A., Snider, C., Yon, J. "A Comparison of Structured Light Scanning and Photogrammetry for the Digitisation of Physical Prototypes", Proceedings of the Design Society, 1, pp. 11–20, 2021. https://doi.org/10.1017/pds.2021.2

[6] Niven, L., Steele, T. E., Finke, H., Gernat, T., Hublin, J.-J. "Virtual skeletons: using a structured light scanner to create a 3D faunal comparative collection", Journal of Archaeological Science, 36(9), pp. 2018–2023, 2009. https://doi.org/10.1016/j.jas.2009.05.021

[7] Georgopoulos, A., Ioannidis, Ch., Valanis, A. "Assessing the Performance of a Structured Light Scanner", International Archives of Photogrammetry, Remote Sensing and Spatial Information Sciences, Vol. XXXVIII, Part 5 Commission V Symposium, pp. 250–255, 2010.

[8] Díez Díaz, V., Mallison, H., Asbach, P., Schwarz, D., Blanco, A. "Comparing surface digitization techniques in palaeontology using visual perceptual metrics and distance computations between 3D meshes", Palaeontology, 64(2), pp. 179–202, 2021. https://doi.org/10.1111/pala.12518

[9] Engelbrecht, J., Philip, L. "Structural Steel and Concrete Analysis Through 3D Scanning", Autodesk University, 2015. [multimedia] Available at: https://www.autodesk.com/autodesk-university/class/Structural-Steel-and-Concrete-Analysis-Through-3D-Scanning-2015

[10] Wiedenmann, E., Scholz, T., Schott, R., Tusch, J., Wolf, A. "First Utilization of Energy Transfer in Structured Light Projection - Infrared 3D Scanner", Key Engineering Materials, 613, pp. 141–150, 2014. https://doi.org/10.4028/www.scientific.net/KEM.613.141

[11] JS Tech Co. "NCTB400C User's guide", 2016.

[12] Lovas, T., Somogyi, Á. J., Simongáti, G. "Laser Scanning Ship Hulls to Support Hydrodynamic Simulations", Periodica Polytechnica Civil Engineering, 66(1), pp. 291–297, 2022. https://doi.org/10.3311/PPci.19353

[13] McDanels, S. "Nondestructive Testing As a Tool in the Space Shuttle Columbia Accident Investigation", In: Fifth International Conference on Condition Monitoring and Machinery Failure Prevention Technologies, Edinburgh, Scotland, 2008, KSC-2008-128.

[14] DeRemer, S. "Short range full-field non-contact structured blue light 3D scanning and photogrammetry for rapid and accurate inspection analysis", In: NASA In-Space Inspection Workshop (ISIW 2014), Houston, TX, USA, 2014, 4c-3.

[15] Somogyi, Á. J., Fehér, K., Lovas, T., Halmos, B., Barsi, Á. "Analysis of Gothic Architectural Details by Spatial Object Reconstruction Techniques", Periodica Polytechnica Civil Engineering, 61(3), pp. 640–651, 2017. https://doi.org/10.3311/PPci.10418

[16] Sengoz, B., Topal, A., Tanyel, S. "Comparison of pavement surface texture determination by sand patch test and 3D laser scanning", Periodica Polytechnica Civil Engineering, 56(1), pp. 73–78, 2012. https://doi.org/10.3311/pp.ci.2012-1.08

[17] Hexagon "SmartScan" [online] Available at: https://www.hexagonmi.com/products/structured-light-scanners/aicon-smartscan (Accessed 18, February, 2022)

[18] AESUB "AESUB white" [online]. Available at: https://aesub.com/en/products/aesub-white/ (Accessed: 18, February, 2022)

[19] 3D Systems "Geomagic Wrap" [online] Available at: https://www.3dsystems.com/software/geomagic-wrap (Accessed: 18, February, 2022)

[20] 3D Systems "Geomagic Design X" [online]. Available at: https://www.3dsystems.com/software/geomagic-design-x (Accessed: 18, February, 2022)

[21] 3D Systems "Geomagic Control X" [online]. Available at: https://www.3dsystems.com/software/geomagic-control-x (Accessed: 18, February, 2022)